

Special properties of overdoped 123 compounds; Cu(2) NQR and Tm NMR of $\text{TmBa}_2\text{Cu}_3\text{O}_x$ at low temperatures

M. A. Teplov, A. V. Duglav, E. V. Kryukov, O. B. Marvin, and I. R. Mukhamedshin

Kazan' State University, 420008 Kazan', Russia

D. Wagner

Bonn University, W-5300 Bonn, Germany

(Submitted 7 July 1995)

Zh. Éksp. Teor. Fiz. **109**, 689–705 (February 1996)

The ^{169}Tm NMR and $^{63}\text{Cu}(2)$ NQR spectra, as well as the spin-spin and spin-lattice relaxation of thulium nuclei, are studied in a series of oriented $\text{TmBa}_2\text{Cu}_3\text{O}_x$ powders with an oxygen content x from 6.9 to 7.0 (in $\Delta x=0.02$ intervals). All the experiments are performed by the spin-echo technique at liquid helium temperatures. Additional measurements of the diamagnetic susceptibility at 1 kHz in a field $H_1 \sim 1$ Oe perpendicular to the c crystallographic axis show that the maximum critical temperature $T_c(\text{onset})=92.2$ K is achieved in the samples with $x=6.90$ – 6.92 . The results of the experiments with the overdoped compounds ($x \geq 6.94$) are consistent with the “ribbon model” of the quasi-one-dimensional spin and charge correlations in CuO_2 planes [O. N. Bakharev, M. V. Eremin, and M. A. Teplov, JETP Lett. **61**, 515 (1995)]. A “disappearance” of 1/3 of the intensity of the Cu(2) NQR signal is discovered when the oxygen content is decreased from 7.00 to 6.98. Phase separation is discussed as a possible cause of this effect. It is theorized that in layers with a reduced concentration of holes in the CuO_2 planes, the mobility of the holes decreases, the fluctuations of the strong internal fields from the spins of the Cu^{2+} ions slow, and the spin echo of the Cu(2) nuclei is not observed due to acceleration of the transverse nuclear relaxation. © 1996 American Institute of Physics. [S1063-7761(96)02602-8]

1. INTRODUCTION

The physical properties of the high-temperature superconductors $\text{RBa}_2\text{Cu}_3\text{O}_x$ ($\text{R}=\text{Y}$ or a rare-earth element) with oxygen indices corresponding to the so-called 90-K plateau depend strongly on the value of x . The maximum critical temperature T_c is observed for $x=x_{\text{opt}}$, when the optimal level of doping of the CuO_2 planes with holes is achieved. According to the evaluations of different investigators, the value of x_{opt} lies in the range from 6.90 to 6.94.^{1,2} The optimal doping level corresponds to the minimum lattice constant c_0 .¹ One characteristic feature of underdoped compounds with $x < x_{\text{opt}}$ is the presence of a gap in the spectrum of magnetic excitations (at 28, 16, 4, and 3 meV for $x=6.92$, 6.69, 6.51, and 6.45, respectively³), which influences many observable properties of superconductors and, in particular, determines the temperature dependence of the NMR and NQR parameters.⁴ Overdoped compounds with $x > x_{\text{opt}}$ have properties which are most similar to those of “conventional” superconductors; however, they exhibit unusual features, some of which can be interpreted as consequences of a phase separation.^{1,5-7} It is known that in overdoped 123 compounds 1) the critical current density decreases,⁸ 2) the concentration of paired current carriers is saturated, although unpaired carriers remain at $T \leq T_c$ (Ref. 9), 3) the application of hydrostatic pressure lowers, rather than raises, the critical temperature T_c (Ref. 10), 4) the magnetic susceptibility in the normal phase increases appreciably with decreasing temperature,¹¹ 5) the thermopower of the polycrystalline substance becomes negative,¹² and 6) the Hall coefficient mea-

sured in a current along the c axis of the crystal also becomes negative.¹³ The last two peculiarities definitely point to the appearance of electronic conductivity.

The purpose of the present study is to use magnetic resonance methods (NQR and NMR) to detect fundamental variations in any parameters of $\text{TmBa}_2\text{Cu}_3\text{O}_x$ (TmBCO_x) superconductors which might shed some light on the reasons for the drastic difference between the properties of overdoped and underdoped compounds having practically identical critical temperatures within the 90 K plateau. The main impetus was the hypothesis that underdoped 123 compounds, unlike overdoped compounds, contain layers of a phase which is not observed in Cu(1) and Cu(2) NMR, but manifests itself indirectly in the NMR properties of the phases observed. This hypothesis is based on the fact discovered some time ago,¹⁴ but hitherto not confirmed, that the intensity of the Cu(1) and Cu(2) NQR signals in YBCO_x decreases by 1/3 when the oxygen index varies from 7.00 to 6.97. We were able to corroborate this fact and to show that the “disappearing phase” is characterized by tetragonal (or pseudotetragonal) symmetry. The results of the investigations of the Cu(2) NQR spectra and the spin-spin relaxation of the Tm and Cu(2) nuclei in overdoped TmBCO_x samples at liquid helium temperatures are consistent with the “ribbon model” of the ordering of the spins and charges in CuO_2 planes.¹⁵

2. EXPERIMENTAL RESULTS

The experiments were performed on six samples of TmBCO_x ($x=6.9$ – 7.0 , $\Delta x=0.02$), which were prepared by a

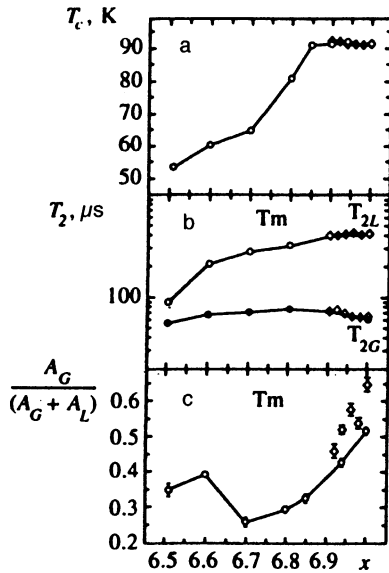


FIG. 1. a) Critical temperature (onset of the transition) of $\text{TmBa}_2\text{Cu}_3\text{O}_x$ superconductors obtained from measurements of the diamagnetic susceptibility at a frequency of 1 kHz (the field $H \sim 1$ Oe is perpendicular to the c axis): unfilled circles—data from Ref. 18, filled diamonds—present work. b) Spin-spin relaxation times of thulium nuclei in oriented TmBCO_x powders at 1.5 K measured in a field $\mathbf{H} \parallel \mathbf{c}$ under the condition $H/\nu = 2\pi/\gamma_a$: filled and unfilled circles—data from Ref. 18, 42–50 MHz, filled and unfilled diamonds—present work, 36–37 MHz. c) Relative number of rapidly relaxing thulium nuclei (T_{2G}) in TmBCO_x samples at $T=1.5$ K: unfilled circles—data from Ref. 18, unfilled diamonds—present work.

solid-phase synthesis technique.¹⁶ Powders mixed with paraffin were oriented in a rotating container in a 20 kOe magnetic field at the melting point of paraffin.¹⁷ Due to the anisotropy of the paramagnetic susceptibility of thulium ($\chi_{a,b} > \chi_c$), the c axes of the powder particles were aligned perpendicularly to the field, i.e., along the rotation axis of the

container, and were fixed when the paraffin solidified. The a and b axes of the powder particles remained randomly oriented in the plane perpendicular to the c axis. The high quality of the powders obtained can be evaluated from the dependence of T_c on the oxygen content (Figs. 1a and 3a) and from the width δ of the $^{63}\text{Cu}(2)$ NQR line (Figs. 2b and 3b). As we see, the optimal doping level is achieved in our samples for $x_{\text{opt}}=6.90-6.92$. All the $\text{Cu}(2)$ NQR and Tm NMR measurements were performed by the spin-echo technique at temperatures from 1.6 K to 4.2 K.

2.1. Spectra

The intensity of the $^{63}\text{Cu}(2)$ NQR spectra was calibrated on the basis of “averaged” NMR spectra of ^{169}Tm (spin $I=1/2$, 100% natural abundance). The compounds TmBCO_x belong to the family of so-called “van Vleck paramagnets.” In the crystalline electric field of these compounds, Tm^{3+} ions ($4f^{12}$, 3H_6 , $J=6$) have a singlet (nonmagnetic) ground electronic state, which is separated from the excited states by an energy of more than 100 cm^{-1} (Ref. 17). The NMR of the singlet-state $^{169}\text{Tm}^{3+}$ ions is “enhanced” by the magnetic hyperfine interaction A_J of the Tm nuclei with $4f$ electrons; therefore, the effective nuclear gyromagnetic ratio

$$\gamma_i = \gamma_I + \frac{2g_J\mu_B A_J}{\hbar} \frac{\sum_n | \langle 0 | J_i | n \rangle |^2}{E_n} \quad (1)$$

is characterized by high sensitivity to the local crystalline-electric-field symmetry. In Eq. (1) the index $i=x,y,z$ denotes the local axes of crystal field, $\gamma_I = -2\pi \cdot 0.354 \text{ kHz/Oe}$ is the gyromagnetic ratio of “free” Tm nuclei, $g_J=7/6$ is the Landé splitting factor, μ_B is the Bohr magneton, $A_J = -\hbar \cdot 393.5 \text{ MHz}$ is the hyperfine coupling constant, and E_n and $|n\rangle$ are the energies and wave functions of the $4f$ subshell in the crystal field (the index 0 refers to the ground singlet with an

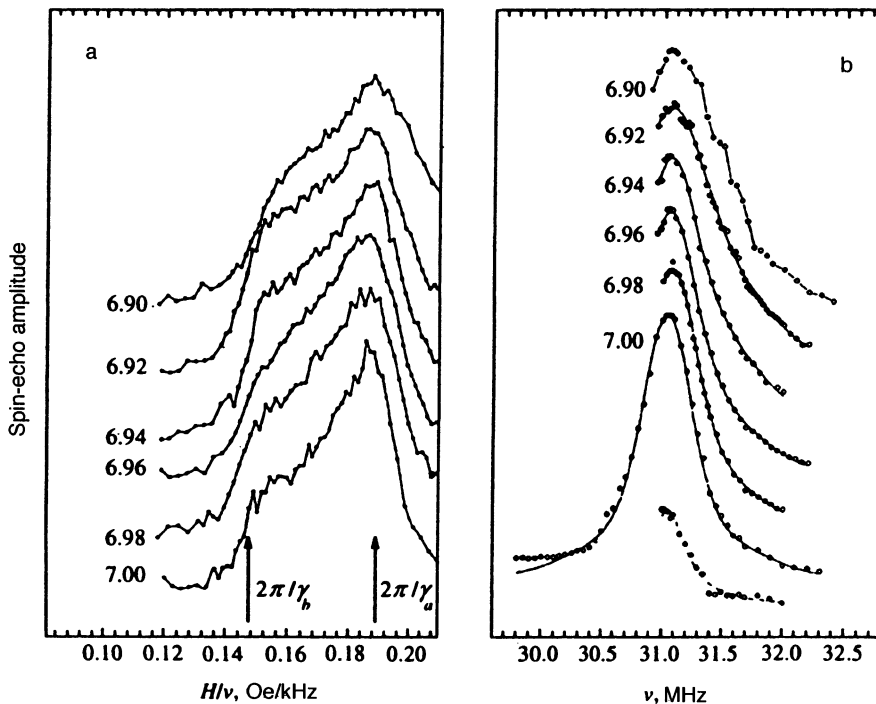


FIG. 2. a) Tm NMR spectra in a field $\mathbf{H} \parallel \mathbf{c}$ at $T=4.2$ K with pulse durations equal to 1.4 and $2.8 \mu\text{s}$ and a delay equal to $20 \mu\text{s}$. b) $^{63}\text{Cu}(2)$ NQR spectra, $T=4.2$ K, pulse durations equal to 2.5 and $5 \mu\text{s}$, delay equal to $24 \mu\text{s}$. To avoid overlapping, the spectra belonging to different values of x have been displaced along the vertical axis.

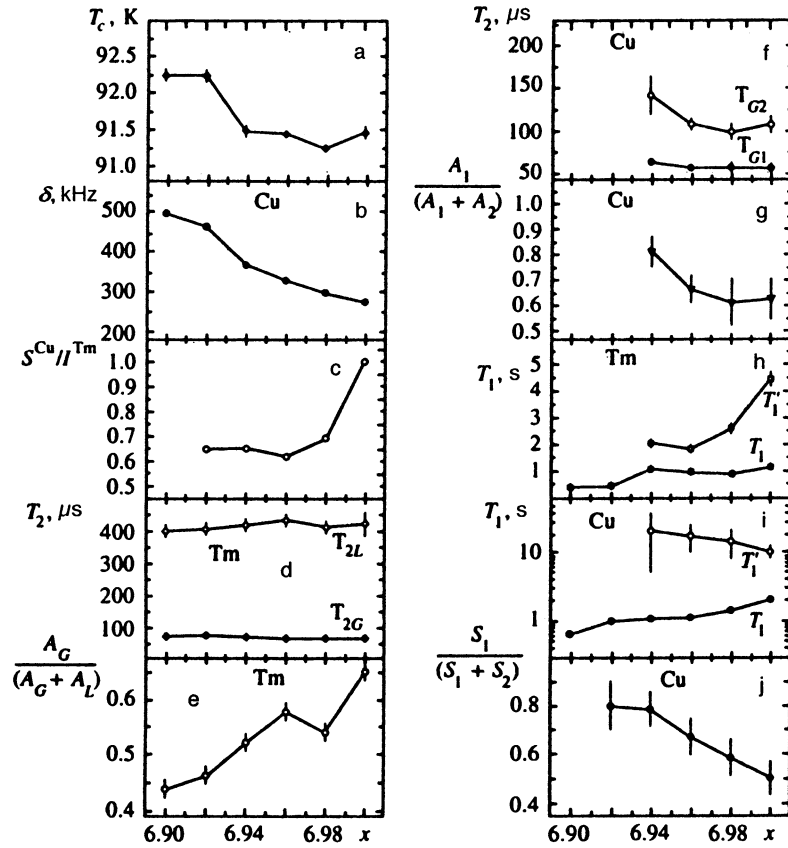


FIG. 3. Dependence of several parameters of the TmBCO_x samples on the oxygen content: a) critical temperature T_c (compare Fig. 1a); b) half-width (at half-maximum) of the $^{63}\text{Cu}(2)$ NQR line, $T=4.2$ K, pulse durations equal to 2.5 and 5 μs , delay equal to 24 μs ; c) ratio of the integrated $^{63}\text{Cu}(2)$ NQR intensity to the peak amplitude (when $H/\nu=2\pi/\gamma_a$) in the ^{169}Tm NMR spectrum, S^{Cu} is the area of half of the $^{63}\text{Cu}(2)$ NQR line (see Fig. 2b), and I^{Tm} is the height of the peak in the spectrum in Fig. 2a; d) spin-spin relaxation time of the Tm nuclei (compare Fig. 1b), duration of the $\pi/2$ pulses equal to 1.2–1.4 μs ; e) relative number of rapidly relaxing thulium nuclei (T_{2G}) (see Fig. 1c); f) spin-spin relaxation time of the $^{63}\text{Cu}(2)$ nuclei, $T=4.2$ K, duration of the $\pi/2$ pulses equal to 2.5 μs ; g) relative number of rapidly relaxing $^{63}\text{Cu}(2)$ nuclei (T_{G1}); h) spin-lattice relaxation time of the Tm nuclei, $\mathbf{H}\parallel\mathbf{a}$, $T=4.2$ K, 36–37 MHz, duration of the $\pi/2$ pulses equal to 1.2–1.4 μs ; i) spin-lattice relaxation time of the $^{63}\text{Cu}(2)$ nuclei, $T=4.2$ K, 36–37 MHz, duration of the $\pi/2$ pulses equal to 2.5 μs ; j) relative weight of the broad ($\Delta_1=500$ kHz) component of the $^{63}\text{Cu}(2)$ NQR line (see Fig. 2b and the explanation in the text).

energy $E_0=0$). Owing to the high sensitivity of the γ tensor to the features of the local environment of the rare-earth ions, Tm NMR is a very convenient method for investigating the structural details of TmBCO_x at low temperatures.¹⁸

It was shown in the preceding experiments^{17,18} that the NMR spectrum of Tm in the ortho-I phase ($x=7.0$) at liquid helium temperatures is described by the spin Hamiltonian $\mathcal{H}_I = -h\sum_i \gamma_i H_i I_i$ ($i=a,b,c$) with the parameters $|\gamma_a/2\pi|=5.3(1)$ kHz/Oe, $|\gamma_b/2\pi|=6.8(1)$ kHz/Oe, and $|\gamma_c/2\pi|=2.20(5)$ kHz/Oe. These values of γ_i provide a graphic picture of what “enhanced NMR” is. For example, the observed gyromagnetic ratio of Tm nuclei in a field $\mathbf{H}\parallel\mathbf{b}$ exceeds the purely nuclear value of γ_I by a factor of 19. As x decreases slightly (within the 90 K plateau), the parameters of the spin Hamiltonian remain approximately constant, and at $x<6.85$ the value of γ_b and γ_c vary strongly, but the effective gyromagnetic ratio γ_a does not depend on the oxygen index and maintains its value down to $x=6.0$. This circumstance enabled us to employ thulium nuclei as an internal reference for calibrating the sensitivity of the spectrometer. Examples of the Tm NMR spectra in a field $\mathbf{H}\parallel\mathbf{c}$, which were recorded at 4.2 K in the $\nu=36\text{--}37$ MHz frequency range, are shown in Fig. 2a. The two features in

the spectra corresponding to the principal values of the γ tensor in the ab plane are marked with arrows. We stress that the low-field shoulder at $H/\nu=0.147$ Oe/kHz is characteristic only of the ortho-I phase, while the peak at $H/\nu=0.189$ Oe/kHz is observed in the Tm NMR spectra of all the phases, including the tetragonal phase ($x=6.0$). The width of such “powder” spectra is determined by the anisotropy of the γ tensor and the degree of orientation of the powders (the inhomogeneous linewidth of the individual crystals plays practically no role); therefore, the spin-echo amplitude of the thulium nuclei at a fixed value of the field $H=2\pi\nu/\gamma_a$ was taken as the quantity characterizing the Tm NMR intensity.

The Tm NMR and Cu(2) NQR intensities in each of the samples were compared during a single experiment at a constant spectrometer sensitivity. We compared the area S^{Cu} of half of the $^{63}\text{Cu}(2)$ NQR line (Fig. 2b) with the amplitude I^{Tm} of the peak in the Tm NMR spectrum, assuming that the value of I^{Tm} measured in a field $H\approx 2\pi\nu/\gamma_a$ is proportional to the total number of Tm nuclei in the sample. The results of our measurements (Fig. 3c) confirm the results obtained in Ref. 14: when x decreases from 7.00 to 6.98, the intensity of the $^{63}\text{Cu}(2)$ NQR line decreases by one-third.

In order to obtain a picture of the form of the “disap-

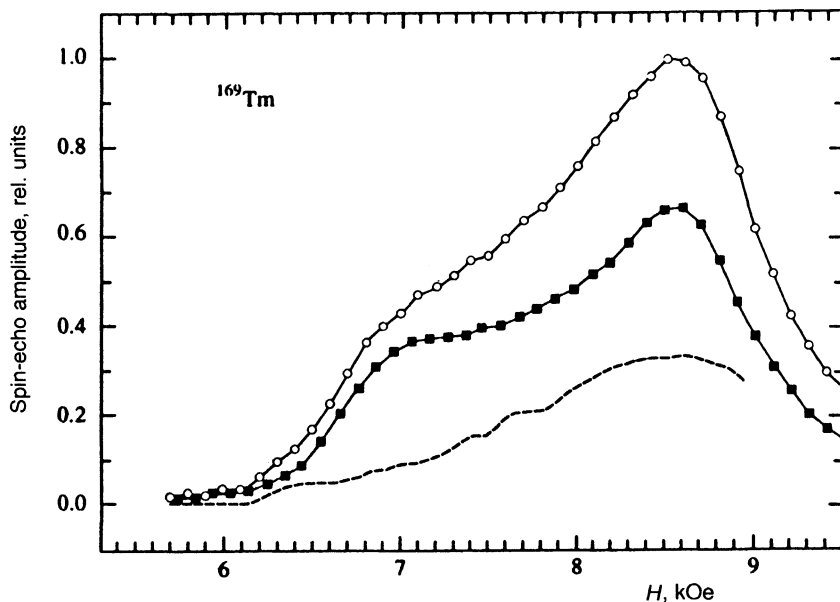


FIG. 4. Example of the decomposition of the Tm NMR spectrum of the TmBCO₇ into components: unfilled boxes—spectrum of a sample with $x=7.0$, 1.5 K, 46 MHz, duration of the $\pi/2$ pulses equal to 1.5 μ s, delay equal to 30 μ s; filled boxes—spectrum of a sample with $x=6.94$, same observation conditions, the amplitude of the peak at $H/\nu = 2\pi/\gamma_a$ was set equal to 2/3; dashed line—the difference $I^{\text{Tm}7.00} - (2/3)I^{\text{Tm}6.94}$ (see explanation in the text).

pearing” contribution to the Cu(2) NQR line, we can find the difference $I^{\text{Cu}7.00} - (2/3)I^{\text{Cu}6.98}$, where $I^{\text{Cu}x}$ denotes the spin-echo amplitudes of the Cu(2) nuclei at equal values of the frequency ν . This difference, which is depicted in the lower part of Fig. 2b, takes the form of a Lorentzian line with the same resonant frequency as the principal line and a half-width at half-maximum $\Delta\nu_{1/2} \approx 200$ kHz. The interesting fact is that the disappearance of 1/3 of the intensity of the copper signal observed when x decreases from 7.00 to 6.98 is accompanied by a change in the shape of the Tm NMR spectrum (Fig. 2a), viz., a decrease in the height of the I^{Tm} peak at $H/\nu = 2\pi\nu/\gamma_a$ relative to the low-field shoulder at $H/\nu = 2\pi\nu/\gamma_b$ (the spectra of the compounds with $x=6.94-6.98$ differ only slightly). We obtain the thulium NMR spectrum corresponding to the “disappearing” phase in the Cu(2) NQR spectrum by finding the difference $I^{\text{Tm}7.00} - (2/3)I^{\text{Tm}6.94}$, where $I^{\text{Tm}x}$ denotes the spin-echo amplitudes of the ^{169}Tm nuclei in identical magnetic fields and the factor 2/3 is set equal to the value for the Cu(2) NQR spectra. The result of this decomposition (Fig. 4) reveals that the spectrum of $I^{\text{Tm}7.00}$, unlike the spectrum of $I^{\text{Tm}6.94}$, contains a tetragonal or pseudotetragonal component (which is depicted by the dashed line), which is very similar to the Tm NMR spectrum of TmBCO_{6.2} in a field $\mathbf{H} \perp \mathbf{c}$.¹⁸ In fact, in this additional component, which distinguishes the spectrum for $x=7.0$ from the spectrum for $x=6.94$, the low-field shoulder at $H/\nu = 2\pi\nu/\gamma_b$, which is characteristic of the orthorhombic Tm centers, is simply absent.

2.2. Spin-spin relaxation

In our earlier experiments with underdoped TmBCO_{*x*} samples at liquid helium temperatures¹⁸ we observed the spin-echo decay kinetics of the thulium nuclei in a field $\mathbf{H} \parallel \mathbf{a}$ of the form

$$A_{\text{Tm}}(2\tau) = A_G \exp\left[-\frac{1}{2} \left(\frac{2\tau}{T_{2G}}\right)^2\right] + A_L \exp\left(-\frac{2\tau}{T_{2L}}\right) \quad (2)$$

and concluded that TmBCO_{*x*} superconductors contain two types of $^{169}\text{Tm}^{3+}$ centers with different nuclear spin-spin relaxation times. Figures 1b, 1c, 3d, and 3e depict the dependence of the times T_{2G} and T_{2L} and the relative concentration $A_G/(A_G + A_L)$ of the rapidly relaxing Tm centers in both the previously studied samples¹⁸ and the new samples on the oxygen index. Figure 5 presents decay curves of the spin-echo signal $A_{\text{Tm}}(2\tau)$ of the thulium nuclei measured on two series of TmBCO_{*x*} samples in a field $\mathbf{H} \perp \mathbf{c}$ under the condition $H/\nu = 2\pi/\gamma_a$. These curves enable us to see how the contribution of the slowly relaxing Tm nuclei behaves as x increases.

The measurements of the spin-spin relaxation of the Cu(2) nuclei at 4.2 K showed that it is much faster in the TmBCO_{*x*} samples with $x \approx 7.0$ than in TmBCO_{6.98} (Ref. 19). This finding can be attributed to the occurrence of an additional interaction between the Cu(2) nuclear spins and the neighboring Tm nuclear spins. Since a sample of TmBCO_{*x*} presumably contains two kinds of Tm spins with sharply different values of T_2 (Fig. 3d), it can be expected that two components with different times would also be discovered in the spin-echo decay $A_{\text{Cu}}(2\tau)$ of the Cu(2) nuclei. The decay of the spin-echo signal of the Cu(2) nuclei at low temperatures is usually described by a Gaussian curve.¹⁹ As our experiments showed, the spin-echo decay curves of the Cu(2) nuclei in the TmBCO_{*x*} samples at 4.2 K are best described by a sum of two Gaussian curves:

$$A_{\text{Cu}}(2\tau) = A_1 \exp\left[-\frac{1}{2} \left(\frac{2\tau}{T_{G1}}\right)^2\right] + A_2 \exp\left[-\frac{1}{2} \left(\frac{2\tau}{T_{G2}}\right)^2\right], \quad (3)$$

where it is assumed that $T_{G1} < T_{G2}$. The results of the treatment of the experimental data are presented in Figs. 3f and 3g. At $x=6.96-7.00$ the value of T_{G2} is the same as that of the single parameter T_G for the Cu(2) nuclei in TmBCO_{6.98}

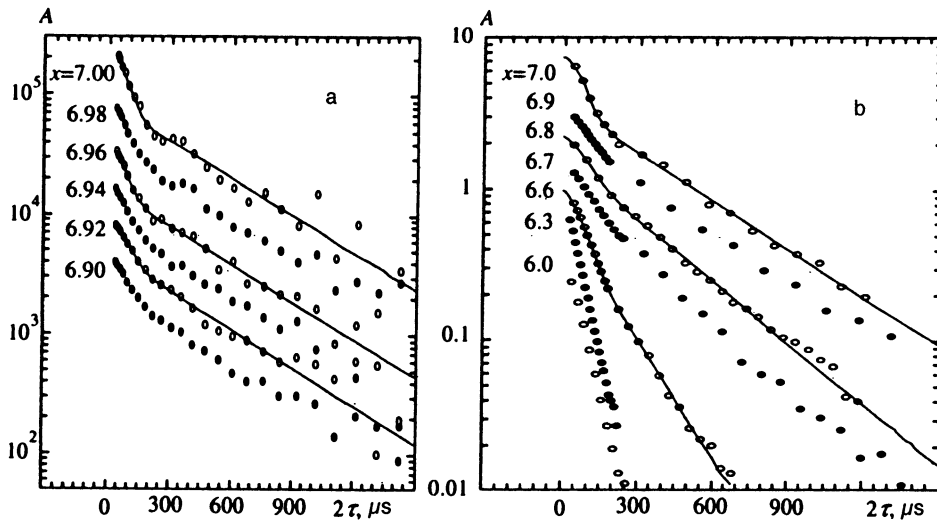


FIG. 5. Spin-echo decay curves of Tm nuclei in oriented TmBCO_x powders in a field $H \parallel a$ at 1.6 K; a) present work, b) data from Ref. 18.

(Ref. 19), while T_{G1} is two times shorter. Another noteworthy feature of the observed two-component relaxation of copper is that the relative content of the rapidly relaxing and slowly relaxing Cu(2) centers is equal to $A_1:A_2=2:1$. We shall discuss this feature below.

2.3. Spin-lattice relaxation

It was previously established^{17,18} that in underdoped samples at low temperatures the relaxation of thulium caused by the paramagnetic copper centers is described by the function $1 - M_t/M_\infty = \exp(-\sqrt{t/T_1})$ (Ref. 18). Such kinetics for restoration of the longitudinal magnetization is characteristic of the case of strong inhomogeneous broadening of the NMR lines, in which there is no nuclear spin diffusion and the nuclear spins impart their energy directly to the paramagnetic centers.²⁰ Experiments with overdoped TmBCO_x samples at 4.2 K showed that the kinetics of the restoration of the longitudinal magnetization of the thulium nuclei are best described by the expression

$$1 - \frac{M_t}{M_\infty} = \exp\left(-\sqrt{\frac{t}{T_1}}\right) \exp\left(-\frac{t}{T'_1}\right) \quad (4)$$

which is also valid for Cu(2) nuclei. The relaxation parameters are presented in Figs. 3h and 3i. As is seen, the value of T_1 for both types of nuclei increases somewhat as x increases from 6.92 to 7.0, pointing to a decrease in the concentration of the paramagnetic centers, i.e., "cleaning" of the samples as they approach the stoichiometric composition.

The relaxation mechanisms of the Tm and Cu(2) nuclei characterized by T'_1 are apparently different. The value of T'_1 for the Tm nuclei increases as x increases from 6.94 to 7.0, and, in addition, it increases as the temperature is lowered from 4.2 K to 1.6 K, i.e., qualitatively, it behaves just like T_1 . Such behavior of the values of T_1 and T'_1 for the Tm nuclei suggests that they are determined by a single mechanism, viz., by a relaxation mechanism involving paramagnetic acceptor centers such as localized Cu²⁺ spins. In the samples with $x \approx 7$ the inhomogeneous Tm NMR linewidth, which is associated with structural defects, probably de-

creases so much that some of the Tm nuclei become capable of relaxing through the same paramagnetic acceptor centers, but along a nuclear spin diffusion channel, rather than directly. Conversely, the value of T'_1 for the Cu(2) nuclei decreases as $x \rightarrow 7.0$. This indicates that an independent relaxation channel not associated with paramagnetic defects appears. It can be assumed that the independent channel is associated with unpaired charge carriers, which, as optical measurements of the conductivity along the c axis of YBCO_x crystals have shown,⁹ appear in the overdoped state and disappear in the underdoped state. The current carriers in the CuO₂ planes can hardly be involved in nuclear relaxation at liquid helium temperatures. In fact even if the concentration of the unpaired carriers had an appreciable value (which is unlikely at $T \ll T_c$), their presence would be detected in the relaxation of the Tm nuclei through the mechanism of the exchange interaction between the rare-earth ions and the copper ions in the CuO₂ planes (which was discovered, for example, in Ref. 21), i.e., would most probably cause correlated variation of the values of T'_1 for the thulium and copper nuclei. Relaxation of the Cu(2) nuclei through the conduction electrons in the CuO chains seems more likely. In fact, in our experiments the relaxation of copper characterized by T'_1 becomes noticeable precisely at the values of x (6.94–7.00) where a negative thermopower is observed for $T > T_c$ (Ref. 12). At the same time, it follows from measurements of the thermopower in an overdoped monodomain YBCO_x crystal²² that the main negative contribution at $T_c < T \leq 250$ K is made by the CuO chains.

3. DISCUSSION

We begin the discussion with an analysis of the data on the spin-spin relaxation of the Tm and Cu(2) nuclei. The short time T_{2G} for Tm nuclei was previously attributed in Ref. 18 to ¹⁶⁹Tm³⁺ centers which appear within regions with a weakly disordered crystal structure, have similar Larmor frequencies, and are coupled by an effective dipole-dipole interaction of the $I_{j+}I_{k-} + I_{j-}I_{k+}$ type, while the long time T_{2L} was assigned to Tm spins in regions with strong disor-

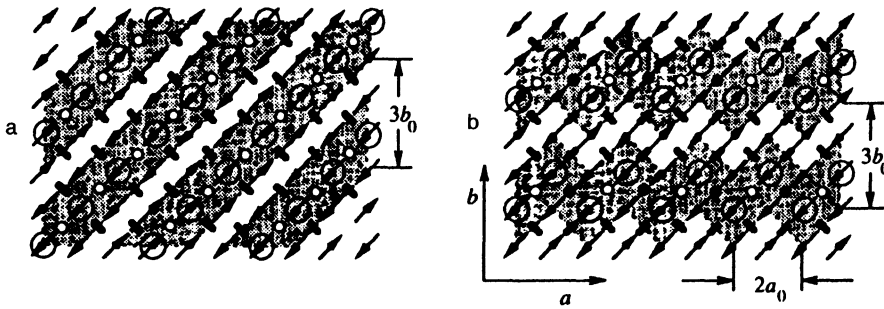


FIG. 6. Two probable ribbon models of the quasi-one-dimensional ordering of the charges and spins in CuO_2 planes (see Ref. 15 and the explanation in the text).

dering. In the case of superconductors with critical temperatures of ≈ 90 K, such an explanation for the large values of T_{2L} cannot be considered satisfactory, since, in view of the increase in T_{2L} observed as the oxygen index increases from 6.8 to 7.0 (Fig. 1b), we would have to assume that the degree of disorder in the crystal lattice increases as the stoichiometric composition is approached. We shall seek an alternative explanation on the basis of the idea that overdoped TmBCO_x compounds have not only an ideal crystal structure with a completely ordered oxygen sublattice in the CuO basal planes, but also an ordered structure of charges and spins in the CuO_2 planes. The existence of the latter is supported both by the observation of two relaxation times T_2 for the thulium and copper nuclei and by the important fact that the number of rapidly relaxing spins in both spin systems is twice as large as the number of slowly relaxing spins. This 2:1 ratio is consistent with the recently proposed "ribbon model" of the quasi-one-dimensional ordering of the charges and spins in CuO_2 planes.¹⁵ In fact, as can be seen from Fig. 6, in both variants of the ordering in the CuO_2 planes there are two types of Cu^{2+} centers, i.e., centers on the edges and along the middle of the ribbons, in a 2:1 ratio. If adjacent CuO_2 planes separated by a distance of 3.3 Å have an identical ribbon structure, it is not difficult to see that this system should also contain two types of Tm^{3+} centers (the projections of their positions onto a CuO_2 plane are illustrated in Fig. 6 by the short thick lines inclined to the right and the left and by the light and dark circles in the same 2:1 ratio. In the experiment (Fig. 3e) such a ratio between the thulium nuclei with short (T_{2G}) and long (T_{2L}) relaxation times is achieved only in the $\text{TmBCO}_{7.00}$ sample with the limiting oxygen content, although it is observed for the copper nuclei already when $x=6.96$. We suggest that this disparity can be caused by violation of the correlation between the ribbon structures of adjacent CuO_2 planes, which plays a decisive role in this system. The correctness of this hypothesis can be supported by the following arguments. First, in the ribbon model the structural correlation of adjacent planes follows, of necessity, simply from the fact that there are two types of Tm^{3+} centers, two being the minimal number of inequivalent sites for the rare-earth ions, which can be realized only when the ribbons have a parallel arrangement. It is not difficult to see that in the case of close packing of the ribbons (as in Fig. 6), their translation in one of the planes of a bilayer relative to another by any vector $n\mathbf{a}=m\mathbf{b}$ ($n, m=0, 1, 2$) does not alter the 2:1 ratio between the concentrations of the different centers, although the structure of the local environment of each

of the Tm^{3+} centers can be altered. In the case of loose packing (as in the underdoped state), the relative displacements of the ribbons $n\mathbf{a}+m\mathbf{b}$ in adjacent CuO_2 planes must ultimately result in violation of the 2:1 ratio for the Tm^{3+} nuclei. Second, the 2:1 ratio between the Tm nuclei is not observed in every $\text{TmBCO}_{7.0}$ sample. In Figs. 1b and 1c the circles depict the results of the experiments in Ref. 18 with samples which were stored at room temperature for 1.5 years before the beginning of the measurements, and the diamonds depict the results obtained on samples with an almost 3-year storage period at room temperature. It can be assumed that the structural correlation of the CuO_2 planes in a bilayer depends to a certain extent on the structural correlation of the overlying and underlying CuO "chain" planes, and the latter correlation, as we know, is achieved by means of the slow diffusion of oxygen only during prolonged annealing at low temperatures. From this standpoint, the different values of $A_G/(A_G+A_L)$ in the two series of samples (Fig. 1c) are naturally attributed to the different annealing times of the samples at room temperature.

If the two types of $^{169}\text{Tm}^{3+}$ centers in the TmBCO_x samples with $x\approx 7.0$ have different values of T_2 , they should certainly produce different NMR spectra. It is shown in Sec. 3 (see Fig. 4) that the Tm NMR spectrum of the $\text{TmBCO}_{7.00}$ sample has two contributions, viz., an orthorhombic contribution (like the spectrum for $x=6.94$) with a weight of $\approx 2/3$ and a tetragonal (or pseudotetragonal) contribution (like the spectrum in Ref. 18 for $x=6.2$) with a weight of $\approx 1/3$. Of course, such decomposition of the spectrum for $x=7.00$ should be considered very rough, but it reveals the main feature of the thulium NMR spectra in a field $\mathbf{H} \parallel c$, which can be also seen in Fig. 2a, i.e., the fact that the relative weight of the peak at $H/\nu \approx 0.189$ Oe/kHz (and therefore the relative proportion of the tetragonal component) increases in overdoped compounds as x increases from 6.94 to 7.00. If it is taken into account that the value of $A_G/(A_G+A_L)$ then tends to 2/3 (Fig. 3e), i.e., A_G/A_L increases to two, it must be assumed that the NMR spectrum of the sample with $x=6.94$ already contains the tetragonal component in an amount approximately equal to the orthorhombic component. We did not perform a detailed analysis of the "powder" Tm NMR spectra in a field $\mathbf{H} \parallel c$; however, it can be seen from the character of the evolution of the shape of these spectra with increasing x that the spectrum for $x=6.94$ occupies an intermediate position with respect to the relative height of the peak at $H/\nu = 2\pi/\gamma_a$ between the spectra for $x=6.85$ and $x=7.0$. This qualitatively confirms the assumption made

above. However, then the tetragonal component in the spectrum for $x=7.00$ is actually not equal to $1/3$, as in Fig. 4, but to $2/3$, and it turns out, as a result, that the rapidly relaxing “edge” Tm ions (i.e., the ions located on the edges of the double ribbon) produce a pseudotetragonal spectrum, while the “medial” Tm ions (the ions along the middle of the double ribbon) produce an orthorhombic spectrum.

Identification of the Tm spectra will help us to select the most probable form of the conducting ribbons in the CuO_2 planes and to understand the cause of the drastic difference between T_{2G} and T_{2L} . It is clear that in a compound with orthorhombic symmetry (such as TmBCO_7) a pseudotetragonal spectrum can be observed only when the local axes of the identical crystalline electric fields in neighboring Tm^{3+} ions can be oriented in the (001) plane in four ways with equal probabilities. This condition is not satisfied in the scheme in Fig. 6a, while in the “staircase” scheme (Fig. 6b) with close packing of the ribbons it is satisfied in two pairs of edge Tm ions from two neighboring ribbons that are near to one another (they are marked in the figure by short thick lines inclined to the right and the left). As for the medial TM ions, in the scheme in Fig. 6a they are all found in identical crystal fields at distances equal to $\sim a_0\sqrt{2}$ from one another, and in the scheme in Fig. 6b the equivalent Tm sites are separated by large distances ($2a_0$ within one ribbon and $3b_0$ between ribbons).

Using the ordering model devised, we can evaluate the relaxation times of the thulium nuclei $T_2 \sim 1/\sqrt{M_{2B}}$ (Ref. 17) and see how they agree with the measured values [here M_{2B} is the contribution to the second moment of the Tm NMR line caused by a dipole-dipole interaction equal to $\sim(I_{j+}I_{k-} + I_{j-}I_{k+})$ between the equivalent Tm nuclei]. In our evaluations we used the formula for M_{2B} in a tetragonal crystal:¹⁷

$$M_{2B} = \frac{1}{16} \frac{\hbar^2}{\gamma^4} \left\{ \frac{1}{16} \gamma_{\parallel}^8 \left[\left(1 - \frac{4\gamma_{\parallel}^2}{\gamma_{\perp}^2} \right) \cos 2\theta - 1 \right]^2 \sum_j (r_j^2 - 3z_j^2)^2 r_j^{-10} + \frac{9}{2} \gamma_{\parallel}^4 \gamma_{\perp}^4 \sin^2 2\theta \sum_j z_j^2 (x_j^2 + y_j^2) r_j^{-10} + \frac{9}{8} \gamma_{\perp}^8 \sin^4 2\theta \left[\sum_j (x_j^2 + y_j^2) r_j^{-10} + \cos 4\varphi \sum_j (x_j^4 - 6x_j^2 y_j^2 + y_j^4) r_j^{-10} \right] \right\}, \quad (5)$$

where $\gamma^2 = \gamma_{\parallel}^2 \cos^2 \theta + \gamma_{\perp}^2 \sin^2 \theta$, and θ and φ are the polar angles of the field \mathbf{H} in the crystallographic coordinate system. In order to be able to compare the calculated values of T_2 with the experimental values obtained in a field $\mathbf{H} \parallel \mathbf{a}$, we set $\theta = \pi/2$, $\varphi = 0$, $\gamma_{\parallel} = \gamma_c$, $\gamma_{\perp} = \gamma_b$, and $a_0 = 3.8 \text{ \AA}$ in Eq. (5), and in the calculation of the lattice sums we restrict ourselves to only equivalent sites within one plane (in Fig. 6 they are denoted by identical symbols). Then the evaluations for the staircase model (Fig. 6b) give $T_2 = 70 \mu\text{s}$ for the edge Tm nuclei and $T_2 = 380 \mu\text{s}$ for the medial nuclei, i.e., the calculated values of T_2 agree not only qualitatively, but also quantitatively with the measured values of T_{2G} and T_{2L} (Fig. 3d). Similar evaluations for a model of the type depicted in Fig.

6a give times equal to $40 \mu\text{s}$ and $110 \mu\text{s}$, which are significantly shorter and differ from one another considerably less than do the experimental values.

As we noted above, in the spin-spin relaxation of Cu(2) nuclei described by Eq. (3) there can also be two different characteristic times: $T_{G1} = 60 \mu\text{s}$ and $T_{G2} = 110 \mu\text{s}$ (Fig. 3f). The latter value corresponds to $1/3$ of the total number of Cu nuclei (Fig. 3g); therefore, it is natural to assign it to the medial Cu(2) spins in a conducting ribbon. This assumption is sufficient for once again choosing the “staircase” ordering scheme. In fact, the value of T_{G2} scarcely differs from the single characteristic time T_G for the Cu(2) nuclei in $\text{TmBCO}_{6.98}$ (Ref. 19). This means that in TmBCO_x the surrounding Tm nuclei do not have any effect on the spin-spin relaxation of the medial Cu(2) nuclei, as the intrinsic values of T_2 for these Tm nuclei are much greater than T_G . A similar situation can arise when the Tm spins closest to the Cu(2) do not include any which occupy equivalent sites and would therefore have identical Larmor frequencies and small values of T_2 . It is seen from Fig. 6 that this situation is realized in the staircase scheme.

After adopting a two-component model for interpreting the spin-spin relaxation of copper, we should naturally attempt to extend it to the Cu(2) NQR spectra. Analysis shows that in the TmBCO_x samples with $x = 6.92 - 7.00$ the shape of the Cu(2) NQR line at 31.05 MHz is best described by a superposition of two Gaussian curves (the solid lines in Fig. 2b) with the mean-square half-widths $\Delta_1 = 500 \text{ kHz}$ and $\Delta_2 = 200 \text{ kHz}$ and a relative intensity of the broader component $S_1/(S_1 + S_2)$, which, like the relative number of rapidly relaxing copper nuclei (Fig. 3g), decreases as the oxygen index increases (Fig. 3j). In the middle of the region of the overdoped state ($x = 6.96$) we have $S_1:S_2 = A_1:A_2 = 2:1$. Considering this ratio once again from the standpoint of the staircase model, we can conclude that the narrow component of the Cu(2) NQR line, whose intensity increases as the TmBCO_x samples approach the stoichiometric composition, is due to the medial copper ions with the long time T_{G2} . As we have already noted, as $x \rightarrow 7.0$, this component undergoes an additional increase (for reasons still unknown), and the values of $S_1/(S_1 + S_2)$ therefore drops below the $2/3$ level in the $x = 6.98 - 7.00$ region.

Summarizing the results of our research, we see that they are consistent with the conception of quasi-one-dimensional ordering of the charges and spins in the CuO_2 planes¹⁵ and, in addition, point to a specific scheme for this ordering of the staircase type (Fig. 6b). If this conception is correct, staircase ordering can occur in all cuprate superconductors containing CuO_2 planes. Therefore, confirmation of this conception can be sought in experimental data pertaining not only to the 123 system, but also to other high- T_c superconducting compounds. Among these experimental findings we mention only the three most important.

1. The observation of a corrugated surface on a cold-cleaved single crystal of YBCO_x (a CuO chain layer) with a period of 13 \AA , which is approximately equal to three times the lattice constant $3b_0$, by means of scanning tunneling microscopy at $T = 20 \text{ K}$ was reported by Edwards *et al.*²³ They attributed the observed corrugations to spin-density waves in

the CuO chains; however, it cannot be ruled out that CuO chains, in which the oxygen atoms are easily displaced from their equilibrium positions, could play the role of a probe for charge-density waves in the CuO₂ planes in this particular case. In any event, the observed period of the corrugations coincides with the value following from the model depicted in Fig. 6.

2. As the recent investigations of the photoemission spectra of Bi₂Sr₂CaCu₂O_{8+x} (Bi2212) showed,²⁴ the conducting CuO₂ planes are characterized by the presence of a c(2×2) superstructure. Such a superstructure can probably be observed, if staircase ordering is realized in the twinned crystals.

3. The geometry of conducting ribbons of the staircase type should place some restrictions on the directions “allowed” for the wave vectors of the current carriers ($\mathbf{k}||[100]$ and $\mathbf{k}||[010]$). This should create gap anisotropy in superconducting cuprates. It has been reported²⁵ that the gap for $\mathbf{k}||[100]$ and $\mathbf{k}||[010]$ in Bi2212 is equal to 20 ± 5 meV and that the gap for $\mathbf{k}||[110]$ is equal to 5 ± 5 meV. According to the model in Fig. 6b, this can simply mean that the concentration of current carriers with $\mathbf{k}||[110]$ and the corresponding density of states at the Fermi level are small.

In all the preceding arguments we essentially utilized only the geometric properties of the ribbon model and totally ignored its magnetic properties. Nevertheless, the question of the magnetic properties of the conducting ferromagnetic ribbons is certainly one of the key issues. The appearance of strong magnetism in the CuO₂ planes should be “detected” at once by the Cu(2) nuclei (the effect may not be manifested in the Tm NMR spectrum, since the Tm³⁺ ion occupies a centrosymmetric position). It is known, for example, that in antiferromagnetic YBCO₆ a field $H_{\text{int}}=80$ kOe directed perpendicularly to the c axis acts on the Cu(2) nuclei.²⁶ The conspicuous absence of any static magnetic effects (anomalies in the magnetic susceptibility or large NMR/NQR shifts due to strong local fields) in our case compels us to assume that the ordering of the charges and spins in a CuO₂ plane can be dynamic, rather than static, by nature. In such a case it would be more correct to speak about one-dimensional or “ribbon” correlations of the spins and charges in CuO₂ planes, rather than about ordering. In Refs. 27 and 28 the correlation time of the hyperfine magnetic field fluctuations in the Cu(2) nuclei in YBCO₇ was evaluated on the basis of experimental nuclear relaxation data: $\tau_c=2 \times 10^{-15}$ s. If we identify this time with the lifetime of a hole on a medial Cu(2) ion and assume that the arrival of a hole at a neighboring Cu(2) site is accompanied by spin flip, we see that, as a result of the very fast fluctuations of the local fields caused by such spin flips of the copper nuclei, the mean local field in the Cu(2) nuclei will be equal to zero, and the transverse relaxation rate

$$1/T_2 = \gamma^2 H_{\text{int}}^2 \tau_c \quad (6)$$

will be small (≈ 600 s⁻¹) in comparison with the relaxation rate resulting from the spin-spin interaction.¹⁾

Thus, under the conditions of rapid hole hopping, the magnetism of the conducting ribbons can have no effect on the Cu(2) NQR characteristics at helium temperatures. How-

ever, as the hole concentration in the CuO₂ planes decreases, the value of τ_c should increase, and this can result in a decrease in T_2 so drastic that observation of the spin-echo signals of the Cu(2) nuclei becomes impossible. We assume that the “loss” of 1/3 of the integrated Cu(2) NQR intensity of TmBCO_x is observed for just this reason when the oxygen index decreases from 7.00 to 6.98 (see Fig. 3f). The 123 system apparently undergoes a phase separation when there is an oxygen deficiency while the optimal hole concentration [about 1/6 per Cu(2) atom] is maintained in most of the volume. At the same time, the hole concentration in the intervening regions, which occupy a small part of the volume, decreases rapidly (the structural defects have the form of layers, i.e., they form in accordance with the basic properties of the layered structure²⁹). To support our conjectures, we recall here the results in Ref. 30, in which inelastic neutron scattering on the 4f states of Ho³⁺ ions in HoBa₂Cu₃O_x and HoBa₂Cu₄O₈ was studied and it was discovered that the crystalline electric field on the Ho³⁺ ions in a small (~10%) part of the volume of the sample has special properties. Interpreting the asymmetric line shapes in the inelastic neutron scattering spectrum of overdoped HoBa₂Cu₃O_{6.97}, Mesot and Furrer³⁰ showed that the asymmetry is attributable to charge fluctuations of the Cu²⁺O^{-2+δ} (ground state) ↔ Cu^{+2+δ}O⁻² (excited state) type in the CuO₂ planes. If it is assumed that the additional broadening of the line of the excited state obtained as a result of treatment of the experimental data ($\Gamma=0.7-0.4=0.3$ meV) is due completely to the finite lifetime of that state τ_c , the lifetime of a hole in a Cu(2) ion can be obtained from the relation $\tau_c = \hbar/\Gamma$: $\tau_c = 2.2 \times 10^{-12}$ s. When the correlation time is such, the transverse nuclear relaxation rate (6) is extremely large (7×10^5 s⁻¹) and the observation of a pulsed Cu(2) NQR signal becomes impossible. A final answer to the question of the reasons for the disappearance of 1/3 of the Cu(2) NQR intensity in our experiments can be given only after additional research. It is perfectly likely that the “depressed” NQR signal of copper can be detected (as in cobalt-doped YBCO₇ samples³¹) over a broad range of frequencies from 6 to 130 MHz at 1.5 K.

Concluding the discussion, we should make two remarks.

1. Although all the experimental results pertaining to the spectra and spin-spin relaxation of Tm and Cu(2) nuclei have been interpreted in this paper in the ribbon model, we do not rule out the possibility of explaining these results in other ways. The ribbon model was used here, because we were able to account for the entire set of findings as a whole without any perceptible contradictions with experimental data obtained by other methods only on the basis of this model.

2. Having given preference to the ribbon model, we should try to predict its most important consequences and list the physical phenomena by which it might be independently confirmed. The most clear-cut support would be provided by the discovery of the superstructure in RBCO₇ compounds of stoichiometric composition by diffraction methods. If such a superstructure exists, why hasn't it been observed? The difficulties in observing it may be due to the short correlation length of the ribbon structure. It hardly exceeds the dimensions of twins, since the boundaries of the twins are charac-

terized by a reduced concentration of oxygen in the CuO basal planes and a reduced concentration of holes in the CuO₂ planes.³² In fact, as follows from the high-resolution electron-energy-loss spectroscopy (EELS) experiments in Ref. 33, in YBCO₇ of stoichiometric composition synthesized by the standard solid-phase technology, the regions with a reduced oxygen concentration can be separated by distances of the order of tens of angstroms. We stress that success in diffraction experiments can be promoted by using samples with the optimal oxygen content corresponding to regular close packing of the ribbons. At smaller and larger values of x the conditions for close packing of the ribbons are violated, and there should be a resultant decrease in the correlation length of the ribbon structure. It has also not been ruled out that low temperatures are needed to observe the superstructure. Here it would be appropriate to mention the work of Wachter *et al.*,³⁴ in which a strong temperature dependence of the depolarization of the light reflected from the surface of a YBa₂Cu₄O₈ single crystal was observed and it was theorized that this effect is caused by the formation of ferromagnetic microregions (such as magnetic polarons or bipolarons) in the crystal at temperatures below 200 K.

The foregoing statements were made to stress that the ribbon correlations in the ordering of the charges and spins in CuO₂ planes are possibly realized only at low temperatures and most probably have a local character, so that "local" methods employing only probes which do not distort the crystal structure, i.e., the main atoms in the crystal lattice, should be used to detect this phenomenon. The most promising local methods are NMR, NQR, and the inelastic neutron scattering spectroscopy of rare-earth ions.³⁰ In the NMR (NQR) spectra of nuclei which have a quadrupole moment we can expect, for example, to observe broadening (or splitting) of lines as the temperature is lowered due to the differences that appear in the intracrystalline electric field gradients at inequivalent sites. We note that the broadening of the Cu(2) NQR lines in YBa₂Cu₃O₇ at low temperatures has already been noted many times in the literature,^{19,35} but the reasons for it have not yet been the subject of a serious analysis.

4. CONCLUSIONS

The ⁶³Cu(2) NQR and ¹⁶⁹Tm NMR spectra of six TmBa₂Cu₃O_x compounds with oxygen concentrations x from 6.9 to 7.0 have been studied at 1.5–4.2 K. The observed form of the spin-echo decay curves of the thulium and copper nuclei can be described most accurately by assuming that in the overdoped compounds ($x > 6.92$) both spin systems contain two kinds of spins with different values for the spin-spin relaxation time T_2 and that the number of rapidly relaxing nuclei ($T_2 = 70 \mu\text{s}$ for Tm and $65 \mu\text{s}$ for Cu) is twice as great as the number of slowly relaxing nuclei ($T_2 = 400 \mu\text{s}$ for Tm and $110 \mu\text{s}$ for Cu). In the Tm NMR spectrum the pseudotetragonal component, which is reminiscent of the spectrum of TmBa₂Cu₃O_{6.2}, can be assigned to the rapidly relaxing centers, and the ordinary orthorhombic component, which resembles the spectrum of the ortho-I phase, can be assigned to the slowly relaxing centers. The ⁶³Cu(2) NQR line shape is best described by a sum of two Gaussian curves.

One of them, which has a mean-square half-width of 500 kHz, can be assigned to the rapidly relaxing copper nuclei, and the other curve (200 KHz) can be assigned to the slowly relaxing nuclei. In general, the experimental results are consistent with the model of quasi-one-dimensional or "ribbon" correlations in the ordering of the spins and charges in the CuO₂ planes.

It has been discovered that the integrated Cu(2) NQR intensity at 4.2 K is 1/3 smaller in the spectra of the compounds with $x = 6.92, 6.94, 6.96,$ and 6.98 than in the spectrum of the sample with $x = 7.00$. This finding confirms the data in Ref. 14, which were obtained in copper NQR measurements at 300 K. The decrease in the Cu(2) NQR intensity by 1/3 as the oxygen index varies from 7.00 to 6.98 apparently arises because the transverse relaxation time of the Cu(2) nuclei becomes excessively short in a certain portion of the volume of the substance with a reduced concentration of holes in the CuO₂ layers.

This research was carried out as part of the Russian "Current Problems in the Physics of Condensed Media" Scientific-Technical Program (the "Superconductivity" Subprogram, project No. 94029) with support from the Ministry of Science and Technical Policy of the Russian Federation. We thank V. A. Atsarkin, M. V. Eremin, A. V. Egorov, H. Lütgemeier, and E. G. Maksimov for discussing the work and offering some critical remarks. The scheme of the experiments described above was inspired to a considerable extent by the ideas advanced in Refs. 34 and 36–40.

¹We note, incidentally, that with such a value of τ_c the maximum rate of motion of a hole along a ribbon $v \sim a_0\sqrt{2}/\tau_c$ is found to be approximately equal to 2.7×10^7 cm/s, which, together with the effective mass of the current carriers m_c , gives a Fermi energy of ≈ 0.2 eV.

- ¹K. Conder, D. Zech, C. Kruger *et al.*, *Physica C (Amsterdam)* **235–240**, 425 (1994).
- ²R. Hauff, V. Breit, H. Claus, *Physica C (Amsterdam)* **235–240**, 1953 (1994).
- ³J. Rossat-Mignod, L. P. Regnault, C. Vettier *et al.*, *Physica C (Amsterdam)* **185–189**, 86 (1991).
- ⁴D. Brinkmann and M. Mali, in *NMR Basic Principles and Progress*, Springer-Verlag, Berlin, 1994, Vol. 31, p. 171.
- ⁵K. Conder, C. Kruger, E. Kaldis *et al.*, *Physica C (Amsterdam)* **225**, 13 (1994).
- ⁶H. Claus, U. Gebhard, G. Linker *et al.*, *Physica C (Amsterdam)* **200**, 271 (1992).
- ⁷A. Mirmelstein, A. Junod, K.-Q. Wang *et al.*, *Physica C (Amsterdam)* **241**, 301 (1995).
- ⁸M. Daeumling, J. M. Seuntjens, and D. C. Larbaleister, *Nature* **346**, 322 (1990).
- ⁹J. Schutzmann, S. Tajima, S. Miyamoto *et al.*, *Solid State Commun.* **94**, 293 (1995).
- ¹⁰W. H. Fietz, R. Quenzel, K. Grube *et al.*, *Physica C (Amsterdam)* **235–240**, 1785 (1994).
- ¹¹J. P. Emerson, R. A. Fisher, and N. E. Phillips, *Physica C (Amsterdam)* **235–240**, 1455 (1994).
- ¹²J. W. Cochrane, G. J. Russell, and D. N. Matthews, *Physical C (Amsterdam)* **232**, 89 (1994).
- ¹³I. Terasaki, Y. Sabo, S. Tajima *et al.*, *Physica C (Amsterdam)* **235–240**, 1414 (1994).
- ¹⁴A. J. Vega, W. E. Farneth, E. M. McCarron, and R. K. Bordia, *Phys. Rev. B* **39**, 2322 (1989).
- ¹⁵O. N. Bakharev, M. V. Eremin, and M. A. Teplov, *Pis'ma Zh. Eksp. Teor. Fiz.* **61**, 499 (1995) [*JETP Lett.* **61**, 515 (1995)].
- ¹⁶M. Buchgeister, P. Herzog, S. M. Hosseini *et al.*, *Physica C (Amsterdam)* **178**, 105 (1990).

- ¹⁷O. N. Bakharev, A. V. Dooglav, A. V. Egorov *et al.*, *Appl. Magn. Reson.* **3**, 613 (1992).
- ¹⁸O. N. Bakharev, A. V. Dooglav, A. V. Egorov *et al.*, in *Phase Separation in Cuprate Superconductors*, edited by E. Sigmund and K. A. Muller, Springer-Verlag, Berlin, 1994, p. 257.
- ¹⁹Y. Itoh, K. Yoshimura, T. Ohomura *et al.*, *J. Phys. Soc. Jpn.* **63**, 1455 (1994).
- ²⁰M. R. McHenry, B. G. Silbernagel, and J. H. Wernick, *Phys. Rev. B* **5**, 2958 (1972).
- ²¹D. N. Aristov, S. V. Maleyev, M. Guillaume *et al.*, *Z. Phys.* **95**, 291 (1994).
- ²²C. K. Subramaniam, H. J. Trodahl, A. B. Kaiser, and B. J. Ruck, *Phys. Rev. B* **51**, 3116 (1995).
- ²³H. L. Edwards, A. L. Barr, J. T. Market, and A. L. de Lozanne, *Phys. Rev. Lett.* **73**, 1154 (1994).
- ²⁴P. Aebi, J. Osterwalder, P. Schwaller *et al.*, *Phys. Rev. Lett.* **72**, 2757 (1994).
- ²⁵Z.-X. Shen, D. S. Dessau, B. O. Wells *et al.*, *Phys. Rev. Lett.* **70**, 1553 (1993).
- ²⁶P. Mendels and H. Alloul, *Physica C (Amsterdam)* **156**, 355 (1988); H. Yasuoka, T. Shimizu, Y. Ueda, and K. Kosuge, *J. Phys. Soc. Jpn.* **57**, 2659 (1988).
- ²⁷O. N. Bakharev, R. Sh. Zhlanov, A. V. Egorov *et al.*, *Pis'ma Zh. Eksp. Teor. Fiz.* **47**, 383 (1988) [*JETP Lett.* **47**, 458 (1988)].
- ²⁸C. H. Pennington, D. J. Durand, C. P. Slichter *et al.*, *Phys. Rev. B* **39**, 2902 (1989).
- ²⁹J. C. Phillips, *Phys. Rev. B* **46**, 8542 (1992).
- ³⁰J. Mesot and A. Furrer, *Physica C (Amsterdam)* **235–240**, 1639 (1994).
- ³¹M. Matsumura, Y. Takayanagi, H. Yamagata, Y. Oda, *J. Phys. Soc. Jpn.* **63**, 2382 (1994).
- ³²S. Blais, O. Thomas, J.-P. S enateur *et al.*, *Physica C (Amsterdam)* **185–189**, 545 (1991).
- ³³Y. Zhu, R. L. Sabatini, Y. L. Wang, and M. Suenaga, *J. Appl. Phys.* **73**, 3407 (1993).
- ³⁴P. Wachter, B. Bucher, and R. Pittini, *Phys. Rev. B* **49**, 13 164 (1994).
- ³⁵J. Freytag, M. Baenitz, S. G artner *et al.*, *Physica C (Amsterdam)* **209**, 59 (1993).
- ³⁶V. Hizhnyakov and E. Sigmund, *Physica C (Amsterdam)* **156**, 655 (1988).
- ³⁷E. L. Nagaev, *Physica C (Amsterdam)* **235–240**, 2427 (1994).
- ³⁸A. Bianconi, *Physica C (Amsterdam)* **235–240**, 269 (1994).
- ³⁹S. Gopalan, T. M. Rice, and M. Sigrist, *Phys. Rev. B* **49** 8901 (1994).
- ⁴⁰K. Gofron, J. C. Campuzano, A. A. Abrikosov *et al.*, *Phys. Rev. Lett.* **73**, 3302 (1994).

Translated by P. Shelnitz